UKAEA-CCFE-CP(21)02

J. Leland, S. Elmore, A. Kirk, H. v/d Meiden. J.
Scholten, S. Allan, J. W. Bradley

Angular Dependence Measurements of Magnum-PSI Plasmas Using MAST-U Flush-Mounted Langmuir Probes

Angular Dependence Measurements of Magnum-PSI Plasmas Using MAST-U Flush-Mounted Langmuir Probes

J. Leland, S. Elmore, A. Kirk, H. v/d Meiden. J. Scholten, S. Allan,
J. W. Bradley

This paper has been submitted to
24th International Conference on Plasma Surface Interactions in Controlled Fusion Devices (PSI), South Korea, 24 - 29 January 2021

Angular Dependence Measurements of Magnum-PSI Plasmas Using MAST-U Flush-Mounted Langmuir Probes

J. Leland[a,b,*], S. Elmore[b], A. Kirk[b], H. J. v/d Meiden[c], J. Scholten[c], S. Y. Allan[b], J. W. Bradley[a]

[a] *Department of Electrical Engineering and Electronics, University of Liverpool, Liverpool, L69 3GJ, UK*
[b] *Culham Centre for Fusion Energy, Culham Science Centre, Abingdon, OX14 3DB, UK*
[c] *DIFFER — Dutch Institute for Fundamental Energy Research, De Zaale 20, 5612 AJ Eindhoven, the Netherlands*

Abstract

Measurements made using flush-mounted Langmuir probes (FMPs) in tokamaks are difficult to interpret when operating at grazing angles of magnetic field incidence due to the effects of sheath expansion on the probe collection area. The Super-X divertor on the upgraded Mega Amp Spherical Tokamak (MAST-U) can have very shallow angles of magnetic field incidence to plasma facing components (1-10°), making the use of conventional flush-mounted probes problematic. A novel probe tip geometry, based on the angled-tip design used successfully on JET and DIII-D, has therefore been used in MAST-U to mitigate sheath expansion effects by increasing the projected probe extent. To verify whether the new design of probe tip allows temperature (T_e) and density (n_e) measurements to be performed accurately at low angles of incidence, a 4-probe array based on this design was used on Magnum-PSI. Parameter scans were made on a range of hydrogen plasmas in conditions comparable to those expected in MAST-U. The measured temperatures and densities were compared to measurements made by the Thomson scattering system on Magnum-PSI. The measured plasma parameters show that the standard MAST-U FMP tip design successfully mitigates the effects of sheath expansion at low angles of magnetic field incidence. The standard MAST-U Langmuir probe also shows an upper operational limit of $\theta = 8°$. This covers the vast majority of expected plasma configurations in MAST-U when running both conventional and Super-X configurations.

Keywords: MAST-U, Langmuir probe, Magnum-PSI, flush-mounted probe, sheath expansion

1. Introduction

Langmuir probes (LPs) are a widely used diagnostic in plasma physics to measure electron temperature (T_e) and density (n_e). LPs in tokamaks are limited to measuring plasma parameters in the edge region due to the extreme nature of the plasmas involved. LPs are thus regularly flush mounted to minimise the incident heat flux to the probe tips and reduce erosion. However, because of the strong dependence of the incidence angle of the magnetic field to the probe surface (θ) on the measured IV characteristics, flush-mounted probes (FMPs) are notoriously difficult to interpret in strongly magnetised plasmas [1].

At grazing angles of incidence, routinely found in tokamak plasma facing components by design, sheath expansion becomes a dominant factor in the determination of the effective collection area (A_{eff}) of the probe [2]. Small uncertainties in θ can therefore have large effects on the amount of sheath expansion included in the fitting of the IV characteristic. Magnetised probe theory is only valid when the projected probe extent is greater than the local Debye length and Larmor radius [3] and can therefore be unusable at small θ.

*Corresponding author
Email address: j.leland@liverpool.ac.uk (J. Leland)

These issues have been previously mitigated on JET[4] and DIII-D by angling the probe tip with respect to the incident magnetic field. This increases the projected probe area and therefore lowers the dependence on small changes of angle. A similar probe tip has been designed for use in the divertor of the MAST-U tokamak at CCFE. An experiment has therefore been carried out with twofold objectives: (a) confirm that the angled-tip design of the probes mitigates the issues caused by grazing angles of incidence, and (b) assess their performance in different regions of plasma parameter space before the upcoming MAST-U experimental campaign. Measurements were taken on the linear device Magnum-PSI at DIFFER, using a 4-probe array with MAST-U-style tips, at a range of plasma parameters and magnetic field configurations. The setup and results of this experiment are presented here as well as a discussion on the consequences for the interpretation of Langmuir probes in MAST-U.

2. Method

2.1. Probes and Probe Electronics

This experiment used the 4-probe array designed for use in the Divertor Science Facility (DSF) at MAST-U [5]. The probe array has 4 separate Langmuir probe tips of different geometry, but only the two closest to the centre of the beam were used - the standard MAST-U Langmuir probe (L) and the smaller probe with half standard area (S) (see fig. 1). The probes are right-trapezoidal in geometry with the surface of the trapezium angled 10° relative to the incident magnetic field. The probes are electrically isolated from each other by a ceramic pin holder, and shadowed from plasma exposure by a graphite shell around the whole assembly. The distances between the probes and the graphite shell were chosen such that the probe's leading edges are shadowed at incidence angles up to 10°.

A specialised mounting assembly was designed and manufactured to hold the DSF probe head in place against the Magnum flat target holder. This target holder was water cooled and could tilt the probes to a range of magnetic field incidence angles (θ).

The voltage sweep on the probes was a 100Hz triangle waveform created by an arbitrary function generator and amplified by a KEPCO 100-4M 100V bipolar operational power supply. The current from the probes was measured by using a dual-channel isolational amplifier to observe the voltage drop across two separate shunt resistors. All of these signals were then digitised by a National Instruments NI PXI-5105 digitiser, with the voltage signal attenuated 10x to be sampled by the digitiser's 10V range. The digitiser sampled at a rate of 100kHz. The amplitude of the voltage sweep was configurable and was therefore varied depending on the plasma parameters being observed, typically from -100V to +10V. The whole system was calibrated by scaling voltage and current values to match the IV characteristic of a 100Ω resistor.

2.2. Magnum-PSI

Magnum-PSI is a linear plasma device capable of producing low temperature ($1 - 10$ eV), high density plasmas ($> 10^{21}$ m^{-}3) in a beam with a FWHM of $\sim 20mm$. The position of the target can be adjusted along the central axis of the beam (z), and rotated at angles to this axis (fig. 2).

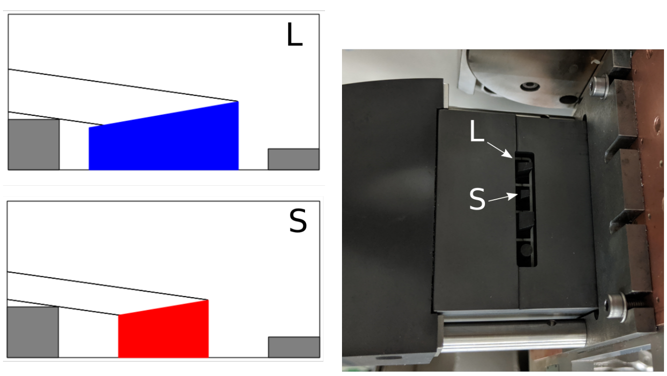

(a) (b)

Figure 1: (a) Probe cross sections showing the geometric area projected along the magnetic field lines for the L and S probes. (b) Photograph showing the DSF probe array installed in Magnum-PSI with the S and L probes labelled.

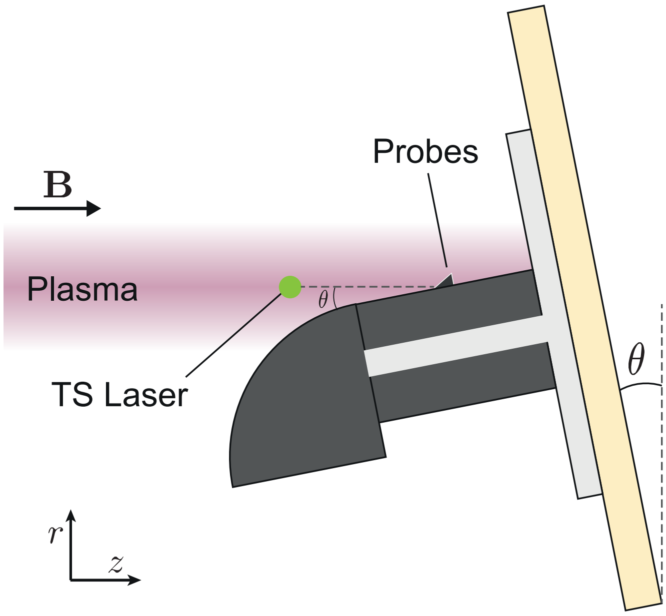

Figure 2: Experimental setup diagram showing relative location of probes and Thomson scattering laser, and θ as the magnetic field incidence angle. r and z correspond to the radial and axial coordinates used throughout.

Density and temperature are not control variables; the input parameters to the source (gas flow and current) and the magnetic field are used in combination to produce different plasmas which are characterised with a well established Thomson scattering system [6]. Peak densities were achieved from 5 $\times 10^{18}$ m^{-3} up to $\sim$1 $\times 10^{21}$ m^{-3}.

Three parameter scans were performed: (a) an incidence angle scans, (b) an axial scan, (c) a density scan. All plasmas measured were hydrogen at a B-field of 0.8T. The angle scan covered the range 0 - 10 ° (as is expected to be the case in the majority of MAST-U plasmas) with the aim of verifying the MAST-U probe's angled-tip design. The axial scan took measurements at different z but with fixed θ, with the Magnum source inputs optimised for maximum T_e. The density scan covered the range 1×10^{19}m^{-3} - 2×10^{20}m^{-3} at a fixed z and θ, to assess to performance of MAST-U LPs in a range of densities expected in the MAST-U divertor. This was achieved by varying the two Magnum source inputs - gas flow and current - between 7.6 - 8.4 standard litres per minute and 100 - 200A respectively.

The TS measurements are made at $z = 0$, and were used as a comparison to the LP measurements. The probe array was rotated parallel to the radial profile measured by the TS system and positioned as close to the TS laser as was possible without intercepting it. The probe holder was aligned on the mounting arm such that the axis of rotation for θ lay inside all probes in the probe array, so as to minimise translation through the beam at different values of θ. Due to a tandem experiment being run by the MAST-U coherence imaging spectrometer, the distance to the TS laser was sometimes extended up to 200mm. Short exposures (5 seconds) were favoured to limit the surface temperature of the graphite components and thus prevent thermionic emission and carbon blooming.

2.3. IV Characteristic Interpretation

For all shots the voltage and current signal was partitioned into individual sweeps. IVs were then sweep averaged, as it was assumed that the plasma was steady state throughout probe exposure, and sweep-direction averaged, to cancel capacitance effects. The uncertainty on each current value was taken as the standard error ($\sigma_{\bar{x}} = \frac{\sigma}{\sqrt{n}}$) of the values being averaged.

A novel combination of probe analysis techniques was employed to minimise temperature overestimation when fitting the measured IV characteristics. The 3-stage method developed on the MAST probe system was used, with the final step being replaced by a temperature minimisation algorithm. All fitting was performed using non-linear least squares. The 3-stage method involves first fitting a straight line to the saturation region of the IV curve (the start of the ion saturation region was decided by eye for each set of shots - either angle scan or density scan - but the final fit parameters were not particularly sensitive to this value). The straight line is then interpolated to generate a starting value for I_{sat}, which is held fixed in a second fit to the whole IV in order to get initial values for the other 3 parameters. Finally a full, freely varying 4-parameter fit is carried out to get final fitting values and uncertainties. However, in this analysis the final fit was replaced by a series of fits extending beyond the floating potential by varying amounts, and returning the minimum from these fits according to a goodness-of-fit parameter. This goodness of fit parameter was set to one of two options: (a) the product of T_e and δT_e (uncertainty on T_e), or (b) the product of T_e, δT_e and $|\chi^2_\nu - 1|$ where χ^2_ν is the reduced χ^2 of the fit. Parameter (a) was used in the majority of cases, unless it was found that prioritising pure temperature minimisation was producing an unphysical fit.

Bergmann's 4-parameter model with Child-Langmuir scaling [7] was selected as the IV characteristic model of choice, as this is known to reduce the overestimation of extracted temperatures [8]. The model is given by

$$\frac{I}{I_{i,sat}} = 1 + a|V|^{\frac{3}{4}} - \exp\left(-V\right) \quad \text{with} \quad V = \frac{e(V_p - V_f)}{k_B T_e} \tag{1}$$

where I is the measured current, $I_{i,sat}$ is the ion saturation current, V_p and V_f are the probe and floating potentials respectively, e is the charge on an electron and k_B is the Boltzmann constant. The sheath expansion parameter, with inclusion of gaps [7], was utilised when calculating a predictive value of a, for both initial fitting parameters and later analysis. This describes the size of the sheath for a completely flush probe and is given by

$$a = \frac{c_1 + c_2 \cot\left(\theta\right)}{\sin^{\frac{1}{2}}\left(\theta\right)} \frac{\lambda_D}{L + g} \tag{2}$$

where c_1 and c_2 are coefficients of the lateral and frontal expansion of the sheath respectively, λ_D is the Debye length, L is the length of the probe and g is the size of the gaps either side of the probe.

Densities were calculated from the fitted parameters using the definition of ion saturation current

$$I_{sat} = n_e Z e c_s A_{eff} \tag{3}$$

where e is the charge on an electron, $c_s = \sqrt{\frac{eZ}{m_i}(T_i + T_e)}$ is the ion sound speed, and A_{eff} is the effective collection area of the probe. The collection area for the shadowed, right-trapezoidal, angled probe tip was derived by extending the derivation of the exposed probe extent to 3 dimensions.

3. Results and Discussion

3.1. Incidence Angle scan

An angle scan varying θ between 0 and 10° was performed for a hydrogen plasma at 0.8T. A set of IV char-

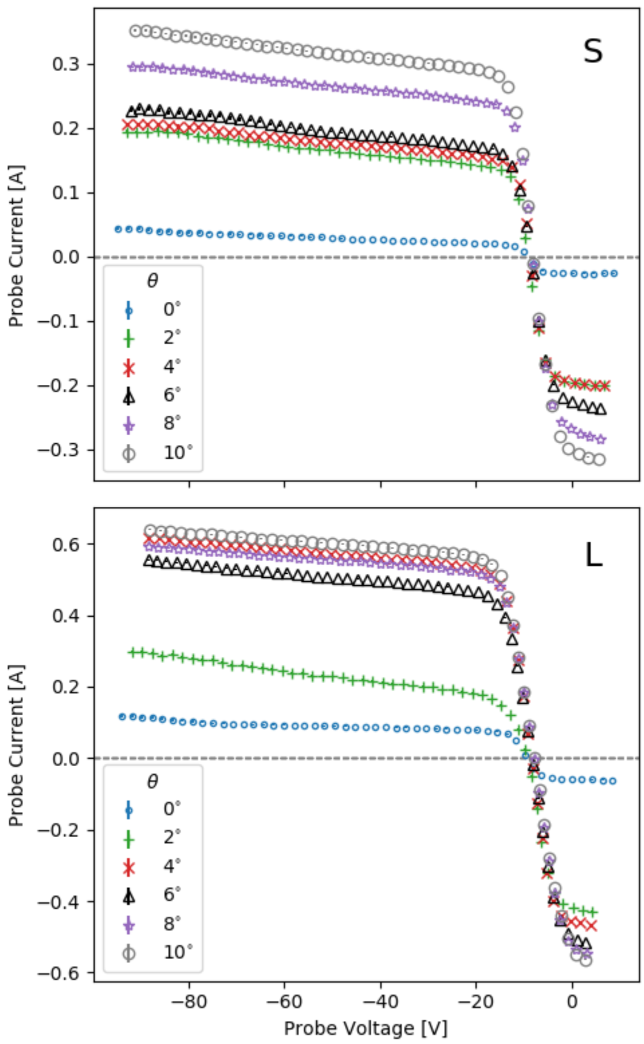

Figure 3: Results of the scan over magnetic field incidence angle for the 0.8T hydrogen plasma. The IV characteristics for the S and the L probe are featured on the top and bottom respectively.

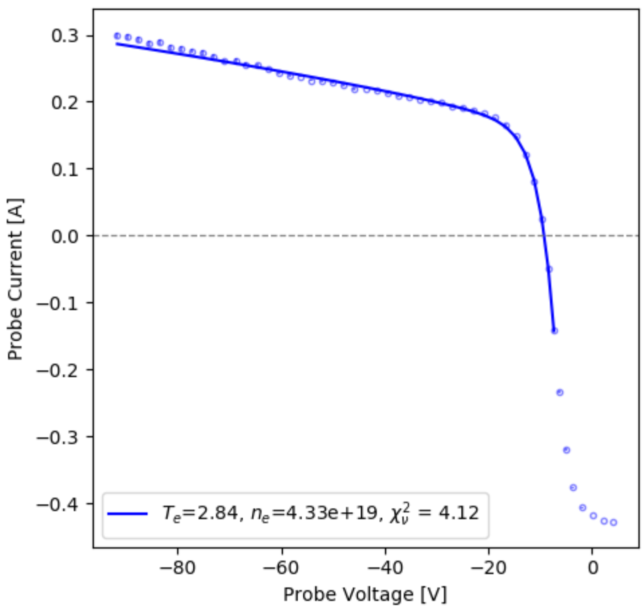

Figure 4: An example IV characteristic (L probe, $\theta = 2°$) with Bergmann's 4-parameter model overlaid. The fit was achieved using the 3-stage method developed on MAST.

acteristics can be seen in fig. 3. Both probes measured higher temperatures and lower densities when compared to TS measurements. The temperature was greater by a factor of 1 - 4 depending on probe, and the density was lower by a factor of 2 - 8. The IV characteristics were found to either fully saturate, or saw very low levels of non-saturation, even at small θ, showing that the design is effectively mitigating sheath expansion effects.

The inferred densities and fitted sheath expansion parameters as a function of incidence angle can be seen in fig. 5. There were two notable trends. Firstly, the density measurements still had a strong θ dependence, with the difference between TS and LP increasing with decreasing θ. The TS value is taken as the linearly interpolated value on the TS profile at the approximate radial probe location. The Thomson scattering measurements did record a slight reduction in density at smaller θ, but this was not large enough to explain this behaviour.

This probably implies that the calculation of A_{coll} - i.e. the geometric area of the unshadowed probe tip projected along the magnetic field - does not accurately describe the probe's actual A_{coll} at small θ.

Secondly, the fitted sheath expansion parameter does not seem to agree with the analytical value. This was calculated from eq. (2) as a function of θ and using the mean TS T_e and n_e for each probe. In the case of the S probe the sheath expansion parameter is almost an order of magnitude larger than the analytical value at $\theta = 10$. Both the S and L probes follow the same rough increasing trend as the analytical case but do not show asymptotic behaviour around $\theta = 0$. This therefore implies that the angled tip probe is successfully eliminating the strong θ dependence at grazing angles of incidence, confirming that the design is working.

As an additional point, the model (eq. (2)) is there-

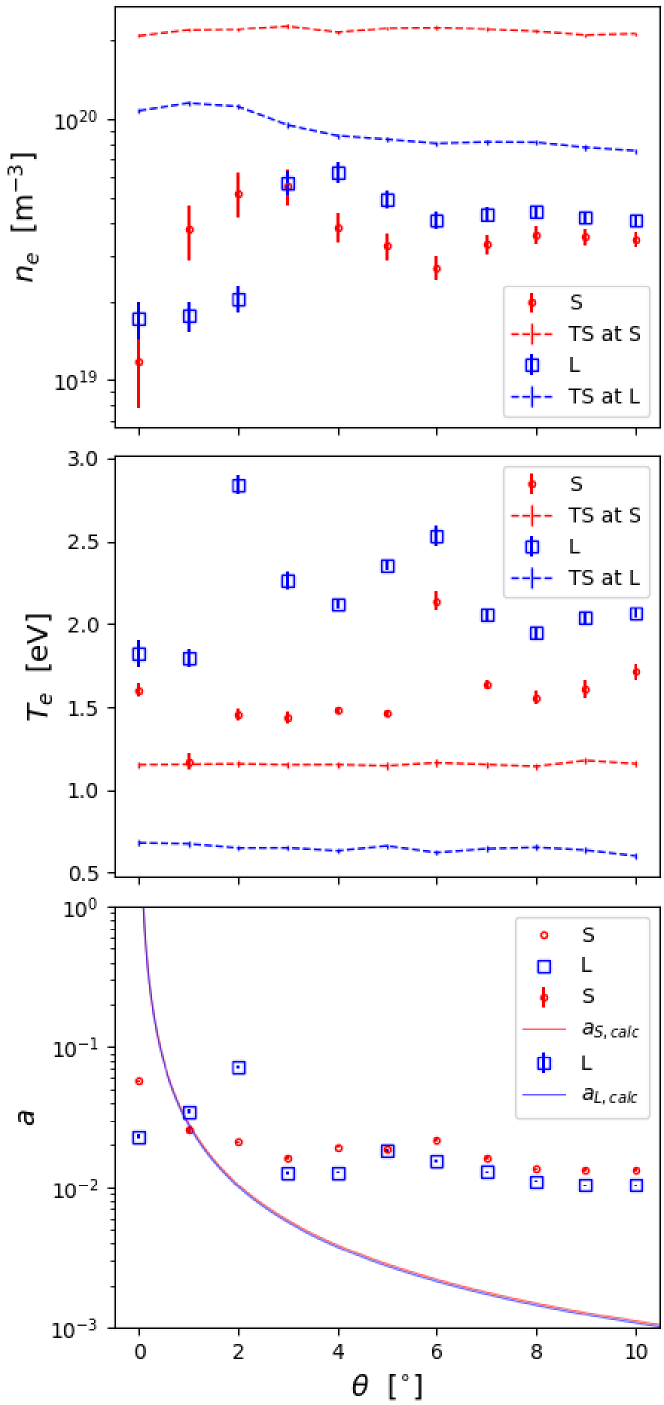

Figure 5: The measured plasma parameters at each value of θ for the 0.8T hydrogen plasma. T_e is temperature, n_e is electron density, and a is the sheath expansion parameter as per eq. (1). The interpolated TS values at each probe's approximate radial position are overlaid for n_e. Bergmann's analytical model for sheath expansion (see eq. (2)), calculated as a function of θ and using the mean TS T_e and n_e for each probe, is overlaid on the sheath expansion plot.

fore ineffective at predicting the sheath size for the angled probe tip. This is not unexpected, as the theory describes a completely flush probe and does not take into account angling the tip or shadowing the leading edge. It would therefore be future work to re-derive this equation with the more complex angled-tip geometry accounted for, so that a correct analytical form with predictive power is known.

3.2. Axial Scan

As mentioned in section 2 the distance of the probes from the Thomson scattering profile was not constant in all cases, so the axial-scan was used to measure the axial density and temperature profiles. This profile may also help with explaining the higher temperatures and lower densities compared to the TS measurements.

The profile width was not expected to change along the beam axis, but a reduction in temperature with distance from the source is expected as energy is radiated away according to particle time-of-flight. The results from this axial scan can be seen in fig. 6. The two probes measured temperatures lower than the TS and density higher than that measured by the TS. This is not unexpected as overestimation of temperature is a common occurrence for Langmuir probe measurements in fusion plasmas, especially at the low temperatures measured by the TS of $\sim 1 - 1.5$ eV at the location of the probe measurements.

The S probe sees a decrease of density towards the source whereas the L probe sees an increase. This may be explained by the arm the probes were mounted to not being strictly aligned with the beam (z) axis, and so 'drooping' downwards when extended to reach smaller z. This translates the probes radially through the beam (in the negative radial direction on the TS profiles on (a) in fig. 6), pushing the more central S probe out towards the wings, and the L probe closer to the centre.

The temperature profiles show opposite profiles to the density however, with the S probe increasing in temperature as density decreases, and the L probe decreasing in temperature towards the source as the density increases. We would expect the temperature to increase as we approach the source, and it may be that this increase in temperature is enough to counterbalance the small decrease in temperature from moving the probe outwards through the radial profile. The larger temperatures on the L probe however, are likely to be the probe measurements drastically overestimating in the very low temperature and low density plasmas at the wings of the profile. This is therefore evidence that the probe system used has an opera-

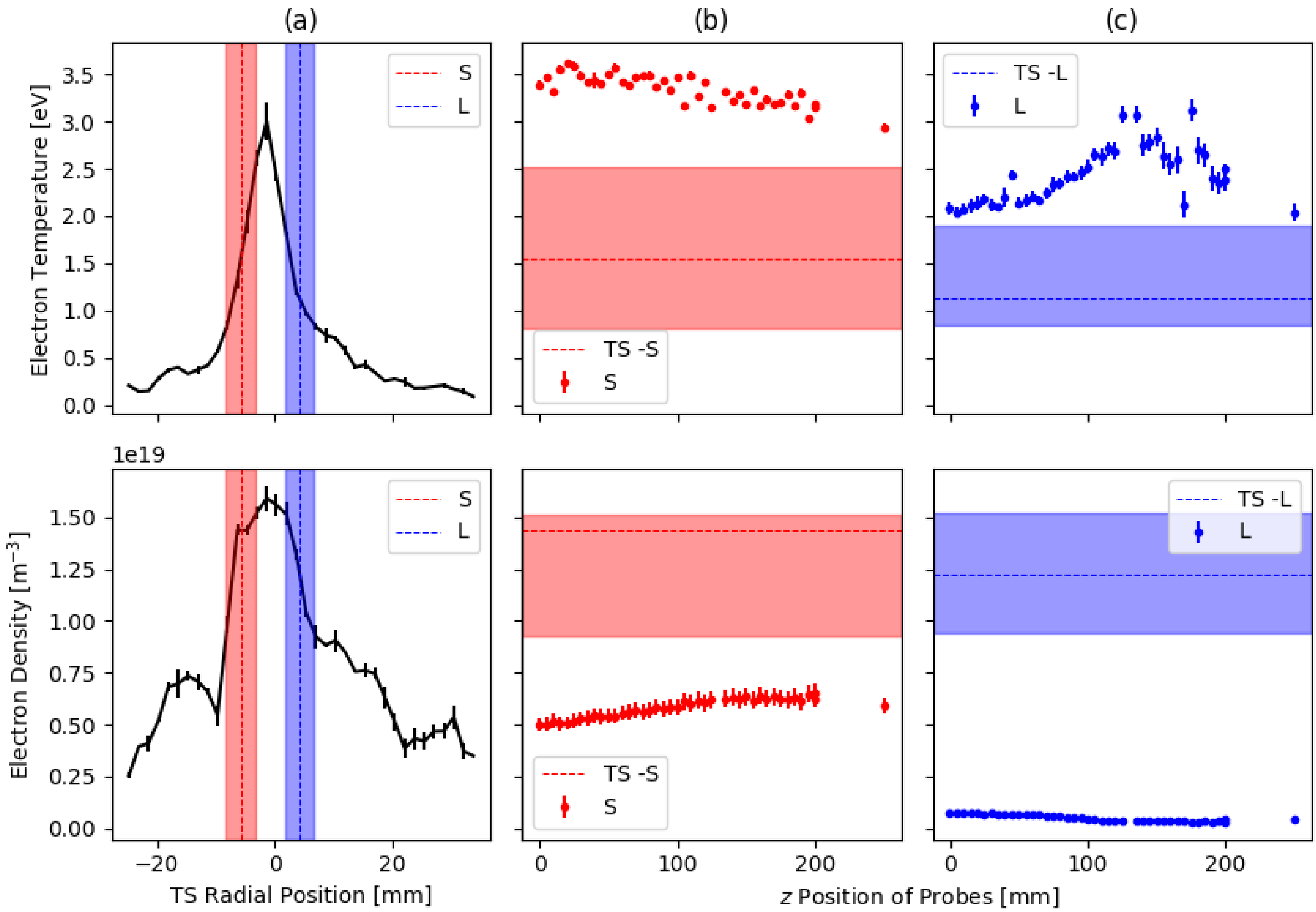

Figure 6: Results of the axial-scan, i.e. the probe measurements taken along the Magnum-PSI beam axis. The top and bottom rows show T_e and n_e respectively, with (a) being Thomson scattering profiles, (b) and (c) being the fit parameters from the S and L probes' IVs respectively. The dotted lines and associated bounds indicate the interpolated Thomson scattering measurement at the position of the S (red) and L (blue) probes and the corresponding uncertainty. The different probe measurements show axial density and temperature profiles with opposite trends, implying that the probes are translating through the radial beam profile with increased z.

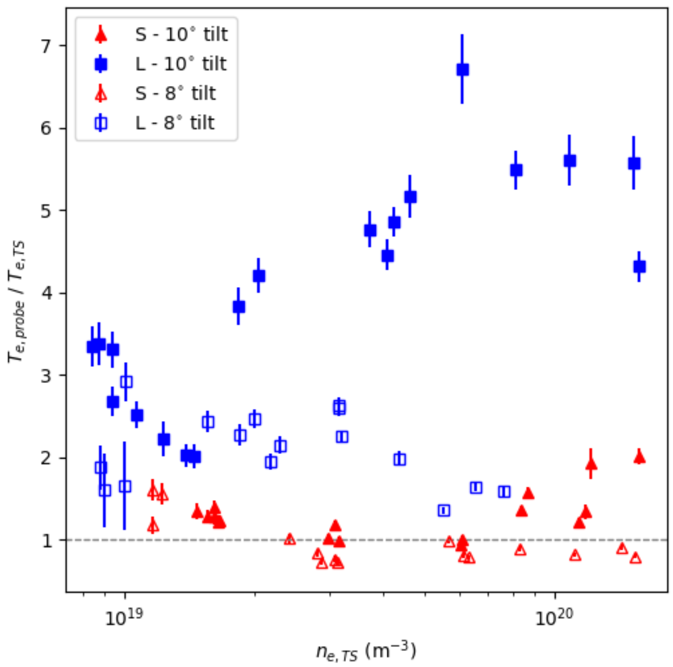

Figure 7: The temperature overestimation factor plotted as a function of TS density at probe radial position, for the S (triangles) and L (squares) probes at $\theta = 8°$ (empty) and $\theta = 10°$ (filled). The shots at $\theta = 10$ on both probes show increasing overestimation of temperature at high densities.

tional density floor of $\sim 7 \times 10^{17}$ m^{-3} and a temperature floor of 1 eV. This does not necessarily imply the same for the MAST-U probe system however, due to the difference in electronics and sweep waveform used.

As most shots were performed between $z = 100 - 200$, which has a broadly flat density and temperature profile, no axial profile corrections were necessary.

3.3. Density Scan

The results from the density scan, performed in order to test the MAST-U Langmuir probe tip's operational parameter space, can be seen in fig. 7. Measurements were taken with the S and L probes at two angles, $\theta = 8°$ and $\theta = 10°$, in plasma densities ranging from $1 \times 10^{19} - 2 \times 10^{20}$.

The ratio between the LP measurements and the TS measurements ($\frac{T_{e,Probe}}{T_{e,TS}}$) did show some dependence on both electron density and θ. The temperature ratio for the S probe at $\theta = 8°$ is roughly constant at ~ 1 across most densities. At $\theta = 10°$ the same is true, except at very high densities where the ratio starts to increase i.e. the LPs are measuring a much larger T_e than the TS. At the lowest densities (9×10^{18} - 2×10^{19}) and at both angles the T_e measured by the S probe is also larger than the TS by up to 50%. For the L probe however there is a much higher temperature measurement ratio for most densities, which for $\theta = 8°$ reduces at higher densities. However for $\theta = 10°$, the ratio is much larger throughout and becomes greater at the highest densities, increasing up to $6\times$ higher than the interpolated TS value at the probe position. The only difference in configuration between the 8 and 10° cases is that the vertical wall face of the trench in which the probes sit is not shadowed by the fore-tile for $\theta > 8.1°$. There is therefore an exposed leading edge in the 10° case which could be sputtering impurities into the plasma around the probes and interfering with the current collection. It would seem therefore, that $\theta > 8°$ is an upper limit on the reliable operational range for the L probe. The L probe is installed throughout the MAST-U divertor, but an upper limit of $\theta = 8°$ would only prevent measurements being made at the very outer probe locations for conventional and Super-x plasma configurations.

4. Conclusions

An experiment has been carried out on Magnum-PSI at DIFFER to both verify the MAST-U probe's angled tip design and to study how it performs within typical conditions expected in the MAST-U divertor.

Results have shown that density measurements are strongly dependent on magnetic field incidence angle, with the density decreasing with decreasing θ compared to the TS measurements. This is likely due to overestimation of the effective collection area of the probe at small θ. Further to this, the observed sheath expansion values on the MAST-U probes do not agree with the predicted value given by Bergmann and Murphy-Sugrue's analytical model. The flat profile of the measured sheath expansion parameters implies that sheath expansion is being mitigated successfully at small θ.

The operational range has been evaluated in terms of temperature measurement compared to the TS system on Magnum-PSI. Results have shown inconsistencies at the upper end of the expected magnetic field incidence angles in MAST-U (10°), with measured temperatures being up to 6 times greater than the TS compared to an equivalent 8° case. This therefore appears to be an upper limit on reliable temperature measurement, particularly at high densities (1×10^{20}) and low temperatures (1eV).

The MAST-U Langmuir probe design has therefore been successfully verified to be working as intended and the probe system will be able to accurately measure temperatures at the small angles of magnetic field incidence expected in the MAST-U divertor. A similar comparison is planned between the Langmuir probes and divertor Thomson scattering systems on MAST-U to confirm these findings.

Funding

This work was supported by the Engineering and Physical Sciences Research Council (EP/L01663X/1) and the University of Liverpool.

References

[1] G F Matthews. “Tokamak plasma diagnosis by electrical probes”. In: *Fusion* 36 (1994), pp. 1595–1628.

[2] A Bergmann. “Two-dimensional particle simulation of Langmuir probe sheaths with oblique magnetic field”. In: *Physics of Plasmas* 1.11 (1994), pp. 3598–3606.

[3] J P Gunn. “The influence of magnetization strength on the sheath: Implications for flush-mounted probes”. In: *Physics of Plasmas* 4.12 (1997), p. 4435.

[4] Raymond David Monk. “Langmuir Probe Measurements in the Divertor Plasma of the JET Tokamak by”. PhD thesis. 1996.

[5] S Elmore et al. “Upstream and divertor ion temperature measurements on MAST by retarding field energy analyser”. In: *Plasma Physics and Controlled Fusion* 54.6 (2012), p. 065001.

[6] H. J. Van Der Meiden et al. “Advanced Thomson scattering system for high-flux linear plasma generator”. In: *Review of Scientific Instruments* 83.12 (2012).

[7] S Murphy-Sugrue. “Numerical Simulations of Probes in Magnetised Plasma”. PhD thesis. University of Liverpool, 2017.

[8] A Podolník et al. “Interpretation of flush-mounted probe current-voltage characteristics using four-parametric fits”. In: *Plasma Physics and Controlled Fusion* 61.10 (2019), p. 105011.